Selectivity of Metallocene-Catalyzed Olefin Polymerization: A Combined Experimental and Quantum Mechanical Study. 1. Nonchiral Bis(cyclopentadienyl) Systems

Manuela Borrelli, Vincenzo Busico,*,† Roberta Cipullo, and Sara Ronca

Dipartimento di Chimica, Università degli Studi di Napoli Federico II, Italy

Peter H. M. Budzelaar*,‡

Department of Inorganic Chemistry (Dutch Polymer Institute), University of Nijmegen, 6500 GL Nijmegen, The Netherlands

Received August 29, 2001; Revised Manuscript Received December 19, 2001

ABSTRACT: Chemo-, regio- and enantioselectivities in the (co-)polymerization of propene and ethene have been measured (in some cases for the first time) for a number of prototypical metallocene catalysts (in combination with methylalumoxane), and compared with those calculated at the DFT level for gas-phase cationic systems. In this paper, the first part of the study, we discuss the *achiral* catalysts Cp_2TiCl_2, Cp_2ZrCl_2, and $Me_2SiCp_2ZrCl_2$. All three catalysts were confirmed to be highly regioselective for propene, in favor of 1,2-insertion. The performance of the titanocene in this respect is truly remarkable (only two misinsertions in 10 000 at −15 °C), whereas that of the two zirconocenes turned out to be worse than generally assumed (two to three misinsertions in 1000), and—quite unexpectedly—nearly identical (both in experiment and calculations), despite the decidedly more open structure of the Si-bridged system. Understandably, in all cases ethene was found to insert faster than propene, but the difference in relative reactivity of the two monomers is particularly dramatic when the growing chain is secondary, which confirms the "dormant" character of the latter for propene. The fair correlation between observed and calculated selectivities suggests that, at least for the systems considered here, solvent and counterion effects, though undoubtedly important, are rather indiscriminate and that olefin insertion is indeed the rate-determining step.

Introduction

The present mechanistic picture of catalytic olefin polymerization (polyinsertion) is an amazing patchwork of bright and dark areas. Elegant and sophisticated applications of ^{13}C NMR to polymer configuration analysis have set the basis for the construction of models which convincingly explain the remarkable enantioselectivity of most catalysts of practical importance.[1] On the other hand, the experimental and theoretical study of the regioselectivity (which results from a delicate interplay between electronic and steric factors) is still fraught with difficulties.[1,2] Last but not least, due to a persisting lack of reliable measurements of active site concentrations and specific insertion rates,[3] the basic reaction kinetics remains obscure; this makes the chemoselectivity also difficult to understand.

The advent in the mid-1980s of homogeneous metallocene catalysts with well-defined precursors[4] represented a breakthrough also in this context. Indeed, their active species can be modeled much more plausibly than those of the classical heterogeneous Ziegler−Natta systems,[5] and it is legitimate to anticipate that theoretical investigations will shed some light on aspects not accessible by experiment.

In our opinion, the implementation of reliable models should start from simple metallocenes, which are now amenable to an ab initio approach, and include some kind of calibration to experimental data. Quite surprisingly, the number of attempts in this direction is very limited. One reason might be that simple metallocenes are much less selective than more recent and sophisticated ones,[1,4] which makes the microstructural analysis of the polymerization products more complicated, and presumably diminishes their appeal, particularly in the experimentalists' view. On the theoretical side, two approaches can be distinguished. On one hand, the polymerization of ethene, as a generic model for olefins, has been studied by sophisticated theoretical methods[6] comprising full quantum-mechanical (QM) treatment of the system, complete geometry optimizations, inclusion of solvent effects and counterions,[7] and even dynamic simulations.[7d,8] These studies have provided a detailed and fundamental insight in the important steps of propagation and chain transfer. On the other hand, the polymerization of propene and higher olefins has mainly been treated using molecular mechanics (MM) or hybrid QM/MM methods.[4b,6,9−13] The main aim there has been to understand the mechanisms regulating stereochemistry and hence to arrive at catalysts with improved performance. However, such approaches are less suited to the study of regioselectivity of propene insertion, or of chemoselectivity in ethene/propene copolymerization, since they do not include the electronic component of the selectivity. There have been very few studies in which propene insertion has been treated fully quantummechanically. Angermund compared insertion of propene with its *re* and *si* faces at a syndiospecific catalyst site.[6b] Moscardi studied the stereochemistry of propene insertion at the C_2-symmetric catalyst *rac*-$Me_2C(3\text{-}t\text{-Bu-1-indenyl})_2ZrR^+$.[14] This is, however, a special case where the ligand exerts both indirect (via the growing chain) and direct effects on the incoming olefin, and the results cannot be easily extended to more

† E-mail: busico@chemistry.unina.it.
‡ E-mail: budz@sci.kun.nl.

10.1021/ma011557h CCC: $22.00
Published on Web 02/28/2002

"normal" metallocenes. The only study which explicitly evaluates regioselectivity and compares ethene and propene insertion at the QM level is by Morokuma et al.[15] They reported a higher propene complexation energy and a higher insertion barrier in Cp_2ZrMe^+ (11.9 vs 6.5 kcal/mol) for propene relative to ethene; also, they found a preference for 1,2- over 2,1-insertion of 4.9 kcal/mol. However, insertion in higher (primary and secondary) alkyl chains was not considered, so that work does not allow us to evaluate the possible "dormant character" of secondary alkyls toward propene,[16,17] one of the important issues in propene homo- and copolymerization.

Thus, we thought it timely to collect a set of experimental selectivity data for ethene and propene (co-)polyinsertion promoted by a number of well-chosen prototypical metallocenes (in combination with methylalumoxane (MAO)), and confront the results with those of a full QM investigation. On doing this, incidentally, we discovered that even from the experimental point of view these "old" catalysts still had a few surprises to deliver.

In the present paper, we describe the outcome of our study for three nonchiral catalysts: $Cp_2TiR]^+$, $Cp_2ZrR]^+$ and $Me_2SiCp_2ZrR]^+$ (the latter modeled as $H_2SiCp_2ZrR]^+$; Cp = h^5-cyclopentadienyl). In a related, forthcoming paper, we will report on a similar study for the chiral, isotactic-selective C_2-symmetric species *rac*-$Me_2Si(1\text{-}Ind)_2ZrR]^+$ (Ind = h^5-indenyl).[18] For each system, we evaluated all possible insertions of ethene and propene at a $L_2Mt-R]^+$ cation, where R was chosen as ethyl (Et) or isopropyl (*i*Pr) to model a primary or secondary alkyl chain, respectively; this allowed us to judge how far one can get without taking "external factors" (like solvent and counterion[4]) explicitly into account.

As we shall see, the agreement between experiment and theory is quite reasonable, which lends support to the calculations, and suggests that the latter can be taken as a sound basis for evaluating kinetic parameters that are not (easily) accessible experimentally, and—more generally—for improving our mechanistic understanding of this fascinating catalysis.

Methods

1. Experimental Methods. (a) Catalysts and Monomers. Cp_2TiCl_2 and Cp_2ZrCl_2 were purchased from Aldrich; $Me_2Si(Cp)_2ZrCl_2$, from Boulder Scientific Co. MAO (10 wt % solution in toluene) was provided by Witco GmbH. Ethene-[1-^{13}C] (Isotec Inc., 99+% isotopic purity) and ethene and propene (Società Ossigeno Napoli, polymerization grade) were used as received.

(b) Propene/Ethene Copolymerizations. All propene/ethene-[1-^{13}C] copolymerizations were run at −15 °C in a 150 mL Pyrex reactor, equipped with a thermostatic jacket, a magnetic stirrer, and a serum cap, according to the following procedure. The reactor, charged under nitrogen with 50 mL of dry toluene (Aldrich) and 2−4 mL of MAO solution, was cooled to −15 °C, evacuated with a membrane pump in order to remove nitrogen, and saturated with propene at the partial pressure of 780 mbar. The appropriate amount of ethene-[1-^{13}C] was injected through the serum cap with a gastight syringe, and once equilibrium conditions were attained, the reaction was started by injecting the appropriate amount of metallocene catalyst (2−6 μmol), previously dissolved in toluene (1.0 mL), from a syringe. The reaction was constantly monitored by means of gas-chromatographic analysis of the gas phase and stopped at low monomer conversion (<10% for propene, <25% for ethene-[1-^{13}C]) by injecting 5 mL of methanol/HCl (aqueous, concentrated) (95/5 v/v). The copolymer was then coagulated with excess methanol/HCl, filtered, washed with more methanol, and vacuum-dried.

Propene/ethene copolymerizations aimed at the determination of the reactivity ratios were carried out using a similar procedure, apart from the fact that the two comonomers were introduced premixed.

(c) ^{13}C NMR Characterization of the Copolymers. Quantitative ^{13}C NMR spectra of all copolymers were recorded with a Varian XL200 spectrometer operating at 50.3 MHz, on 100 mg/mL solutions in tetrachloroethane-1,2-d_2 at 120 °C. Conditions: 5 mm probe; 76° pulse; acquisition time, 1.2 s; relaxation delay, 1.2 s; 20−30K transients. Resonance assignment was based on the literature.[19] The reactivity ratios were determined from the diad and triad compositions of copolymers at natural isotopic abundance, according to the method of ref 20.

2. Calculations. All calculations were carried out with the GAMESS−UK program.[21] Geometries were optimized at the B3LYP level[22] using the 3-21G basis set[23] on the alkyl and olefin, sto-3g on the ligands,[24] and LANL2DZ (small-core pseudopotential) on the metal atom.[25,26] The geometrical parameters for the alkyl and olefin were fully optimized, but several geometric constraints were used for the ligand geometries, as described below. Using a larger basis set and removing geometric constraints would have been feasible for these systems, but not for the $H_2Si(1\text{-}Ind)_2ZrR]^+$ one to be discussed in the next paper, so we decided to use this small basis set throughout for consistency.[27]

For the Cp_2Ti and Cp_2Zr systems, we assumed two identical Cp rings, each with local C_{5v} geometry; movement of each ring relative to the metal was not restricted. For the H_2SiCp_2Zr system, the two Cp groups were assumed to be identical and each with local C_s symmetry; again, movement of each ring of the ligand relative to the metal was unrestricted.

Olefin complexation by the three systems studied is very "soft", and a large number of shallow local minima were found. In the tables, we included only the energies of the lowest-energy minima, even where these do not directly correspond to the geometries for the insertion transition states. As discussed later, the olefin complexation energy does not affect the predicted product distribution anyway.

Zero-point energy (ZPE) corrections were not included.[28] Rough estimates of combined solvation/counterion effects were made as described later. Table 1 shows the relative energies of all relevant species before and after this correction. Table S1 (see Supporting Information) contains total energies of all species studied.

Results and Discussion

1. Experimental Measurements of Selectivities. Although homogeneous olefin polymerization catalysts based on Cp_2MtX_2 complexes (Mt = Ti, Zr; X = halogen, alkyl or aryl) have been in the literature since the mid 1950s,[29] little is known about their selectivity for propene. In a now classical paper,[30] Ewen reported that the polypropylene prepared with Cp_2TiPh_2/MAO (Ph = phenyl), which is atactic for polymerization temperatures T_p > 0 °C, becomes predominantly isotactic at lower T_p (fraction of *meso* diads, [*m*] = 0.85 at T_p = −45 °C), as a result of chain-end control (1,3-*like* asymmetric induction). The Zr homologue has a similar behavior, although the limiting stereoselectivity is somewhat lower. Both catalysts are considered to be highly regioselective, because no resonances indicative of regioirregular enchainments have been detected by ^{13}C NMR in the polymers produced; however, it has to be kept in mind that, due to the comparatively poor sensitivity of this spectroscopy, the threshold for the detection of chain defects in polymers at natural ^{13}C abundance is rather high (somewhere between 0.1 and 1 mol %, depending on the experimental setup and on the specific sample analyzed).[1] The nature of the chain ends proves

Table 1. Relative Energies (kcal/mol) for Ethene and Propene Complexes and Insertion Transition States

		Cp_2Ti		Cp_2Zr		H_2SiCp_2Zr	
system		gas phase	corrected[a]	gas phase	corrected[a]	gas phase	corrected[a]
$L_2MtEt]^+$	(ethene)	−3.7	6.0	−11.9	6.0	−16.2	6.0
	ethene TS	−1.3	8.4	−9.2	8.7	−10.9	11.3
	(propene)	−5.6	5.1	−13.5	5.3	−15.2	8.0
	propene TS 1,2 *anti*	−0.1	10.6	−7.8	11.1	−9.7	13.5
	propene TS 1,2 *syn*	3.6	14.3	−3.4	15.5	−5.3	17.9
	propene TS 2,1 *anti*	4.7	15.4	−3.4	15.4	−5.5	17.7
	propene TS 2,1 *syn*	5.2	15.9	−2.8	16.0	−4.6	18.6
$L_2Mt\text{-}i\text{Pr}]^+$	(ethene)	−1.4	8.3	−10.1	7.8	−13.1	9.1
	ethene TS	(−1.4)[b]	(8.3)[b]	−9.4	8.5	−10.9	11.3
	(propene)	−3.4	7.3	−13.0	5.9	−14.1	9.0
	propene TS 1,2	4.6	15.3	−4.8	14.0	−6.2	17.0
	propene TS 2,1	6.0	16.7	−3.6	15.3	−5.4	17.7

[a] Adjusted for solvation/counterion effects (see text). [b] No TS found, nearly barrierless.

Scheme 1. Definition of Kinetic Constants for Propene Homopolymerization (P = Polymer Chain)

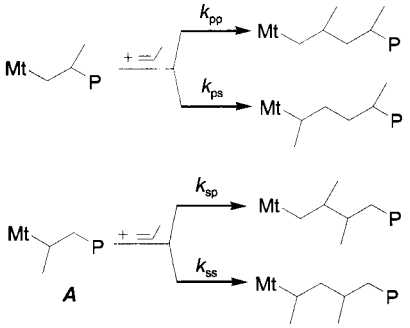

that the predominant propene insertion mode is 1,2 (primary).[1] Even less is known about bridged unsubstituted bis(Cp) catalysts, which is surprising, because *ansa*-Cp_2MtX_2 complexes can be regarded, at least formally, as the ancestors of all substituted stereoselective *ansa*-metallocene catalysts developed in the last two decades.[4] For most of the latter, the regioselectivity is only moderate (≈1 mol % of isolated 2,1-insertions), which has been traced to the wider opening of the catalyst "mouth" induced by the interannular bridge.[1,4]

In propene/ethene copolymerization, it has been reported that Cp_2TiCl_2 and Cp_2ZrCl_2 have a tendency toward comonomer alternation.[31] However, the vertical drop of catalyst productivity and of copolymer average molecular mass with increasing propene content in the feed is a severe drawback for application.

For this investigation, we first measured precisely the regioselectivity for propene of the three catalyst systems Cp_2TiCl_2/MAO, Cp_2ZrCl_2/MAO, and $Me_2SiCp_2ZrCl_2$/MAO, by applying a method based on the ^{13}C NMR microstructural characterization of propene/ethene-[1-^{13}C] copolymers at low ethene-[1-^{13}C] content.

We have already introduced the principles of the method in ref 2. Suffice it to recall here that, in predominantly 1,2-propene polymerization, occasional 2,1-insertions strongly slow the subsequent propene insertion step, in consequence of the steric congestion at a catalytic center bearing a growing polypropylene chain with a 2,1-last-inserted unit. For a number of *ansa*-zirconocene catalysts, the ratio of specific rates k_{sp}/k_{pp} (for definition, see Scheme 1) was estimated[16] to be—typically—in the range $10^{-2} \div 10^{-3}$, which justifies the attribution of "dormant" proposed for species **A** of Scheme 1. On the other hand, it is also well-known that, due to its low steric hindrance, ethene reacts with the dormant chains much faster (>10^2 times) than propene;[2] this means that, in a propene/ethene copolymerization, already at very low ethene/propene feeding ratio, practically all 2,1-propene insertions are followed by an ethene one. Therefore, in the ^{13}C NMR spectra of the resulting copolymer, the resonances of ethene units between two propene units with opposite enchainment can be taken as markers of the propene regioerrors. Of course, if ethene-[1-^{13}C] is used instead of ethene at natural isotopic abundance, the sensitivity of ^{13}C NMR is increased by a factor 50, which means that the threshold for the detection of the regiodefects is lowered correspondingly (down to ≈0.02−0.002 mol %).

We have already reported on the application of the above method to propene polymerization promoted by a few representative C_2-symmetric and C_s-symmetric *ansa*-zirconocene catalysts.[2,32] The protocol requires the preparation of a series of propene/ethene-[1-^{13}C] copolymers with increasing ethene-[1-^{13}C] content, and their microstructural characterization by means of ^{13}C NMR. The mole fraction (Q_{sE}) of ethene-[1-^{13}C] units following a 2,1-propene unit is then plotted against total ethene-[1-^{13}C] mole fraction (Q_E), and the limiting value of the asymptotic curve (for $Q_E \rightarrow 1$) can be taken as the fraction of 2,1-insertions in propene homopolymerization (i.e., as the ratio k_{ps}/k_{pp}, Scheme 1).

Three such plots for the catalyst systems Cp_2TiCl_2/MAO, Cp_2ZrCl_2/MAO, and $Me_2SiCp_2ZrCl_2$/MAO at T_p = −15 °C (a temperature at which chain transfer and 2,1-to-3,1 isomerization[1,4] are slow enough to neglect the occurrence of chain ends and of 3,1 units in the evaluation of the ^{13}C NMR spectra) are shown in Figure 1 (experimental data from Table 2). In all three cases, the experimental curves are well fitted by a standard "saturation" function:

$$Q_{sE} = k_1 Q_E/(k_2+Q_E) \qquad (1)$$

The best-fit values of k_1 (= k_{ps}/k_{pp}) are given in the first row of Table 3.

If, on one hand, it is confirmed that the regioselectivity of the titanocene is extremely high (two 2,1-insertions every 10 000), that of the two zirconocenes, on the other hand, is much worse (two to three 2,1-insertions every 1000). This is somewhat surprising, in the sense that the fraction of regiodefects in the homopolymers made with the latter catalysts is, at least in principle, high enough for ^{13}C NMR detectability. In practice, however, due to the substantial stereoirregularity of such polymers, the weak resonances of the regioirregular sequences are very broad; this apparently

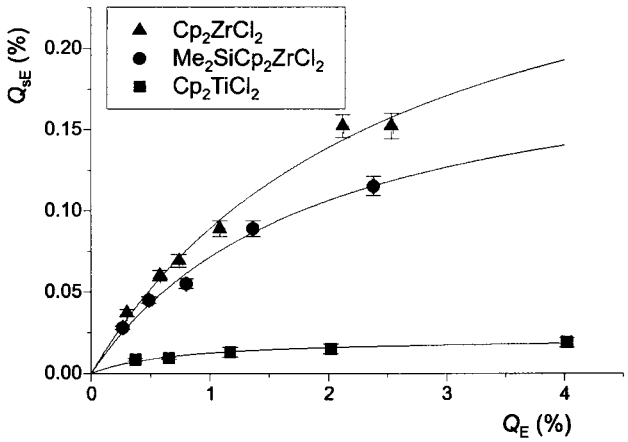

Figure 1. Mole fraction of 2,1-propene units followed by ethene units (Q_{sE}) vs ethene content (Q_E) in propene/ethene-[1-^{13}C] copolymers prepared at −15 °C.

Table 2. ^{13}C NMR Results for the Propene/Ethene-[1-^{13}C] Copolymers

[E]/[P] × 10^3 [a]	Q_E (mol %)[b]	Q_{sE} (mol %)[c]
	Cp_2TiCl_2/MAO	
1.40	4.02(3)	0.019(3)
0.65	2.02(2)	0.015(3)
0.35	1.17(2)	0.013(3)
0.18	0.65(2)	0.0095(5)
0.095	0.369(12)	0.0085(9)
	Cp_2ZrCl_2/MAO	
1.5	2.53(2)	0.152(8)
1.4	2.12(1)	0.151(7)
0.74	1.08(1)	0.089(5)
0.56	0.737(5)	0.069(4)
0.37	0.597(3)	0.060(3)
0.19	0.299(2)	0.037(2)
	$Me_2SiCp_2ZrCl_2$/MAO	
5.57	2.38(1)	0.115(6)
3.00	1.36(9)	0.089(5)
1.79	0.799(5)	0.055(3)
1.00	0.484(4)	0.045(2)
0.64	0.265(2)	0.028(1)

[a] E = ethene; P = propene; in liquid phase, estimated from the composition of the gas feed according to ref 49. [b] ^{13}C NMR mole fraction of ethene units in the copolymer. [c] ^{13}C NMR mole fraction of 2,1-propene units followed by ethene units (referred to the total propene unit content).

prevented their detection in earlier NMR studies. It is also worth noting that the introduction of a Me_2Si bridge has practically no effect on the regioselectivity in the case considered here.

The propene/ethene-[1-^{13}C] copolymerization data can also be used to gain some insight into the chemoselectivity of the process. Indeed, it can be demonstrated[33] that the following linear relationship holds

$$Q_{pE}/Q_{sE} = (k_{pE}/k_{sE})(k_{sp}/k_{ps}) + (k_{pE}/k_{ps})[E]/[P] \quad (2)$$

where Q_{pE}/Q_{sE} is the ratio of ethene-[1-^{13}C] units following a 1,2- or 2,1-propene unit, respectively; [E]/[P] is the comonomer feeding ratio in the reacting (liquid) phase; the specific rates k_{xy} are as defined in Schemes 1 and 2.

Experimental plots of Q_{pE}/Q_{sE} vs[E]/[P] (Table 2) for the three investigated catalyst systems are shown in Figure 2. The data are well interpolated by eq 2, for the best-fit values of k_{pE}/k_{ps} and $(k_{pE}/k_{sE})(k_{sp}/k_{ps})$ reported in Table 3 (rows 2 and 3). From the former ratio, and the previously determined k_{ps}/k_{pp}, one can immediately derive k_{pE}/k_{pp}, which gives the preference for ethene over 1,2-propene to insert after a previous 1,2-propene unit. Dividing k_{pE}/k_{ps} by $(k_{pE}/k_{sE})(k_{sp}/k_{ps})$ gives the same preference after an occasional 2,1-propene insertion, i.e., the ratio k_{sE}/k_{sp}. From the results, which are also given in Table 3 (rows 4 and 5), it appears that the decrease of steric congestion at the catalytic metal along the series $Cp_2TiR]^+ - Cp_2ZrR]^+ - Me_2SiCp_2ZrR]^+$ (see following section) results in a corresponding, progressive fade of the chemoselectivity for ethene. In all cases, however, it is confirmed that ethene inserts much faster than propene at a chain with a 2,1-last-inserted propene unit ($2.8 \times 10^2 \leq k_{sE}/k_{sp} \leq 3.0 \times 10^3$).

Table 3. Estimates of Chemo- and Regioselectivity, Based on the ^{13}C NMR Characterization of Propene/Ethene Copolymers

	Cp_2TiCl_2/MAO	Cp_2ZrCl_2/MAO	$Me_2SiCp_2ZrCl_2$/MAO
$k_{ps}/k_{pp} \times 10^3$	0.22(2)	3.1(4)	2.1(3)
$k_{pE}/k_{ps} \times 10^{-4}$	13(1)	0.59(7)	0.22(3)
$(k_{pE}/k_{sE})(k_{sp}/k_{ps})$	44(7)	6.3(6)	8.0(9)
k_{pE}/k_{pp}	29(3)	19(3)	10(2)
$k_{sE}/k_{sp} \times 10^{-3}$	3.0(5)	0.94(14)	0.28(5)
$r_E = k_{EE}/k_{EP}$	21(1)	7.3(3)	2.1(1)
$r_P = k_{PP}/k_{PE}$	0.020(1)	0.0365(5)	0.19(1)

Scheme 2. Definition of Kinetic Constants for Propene/Ethene Copolymerization (P = Polymer Chain)

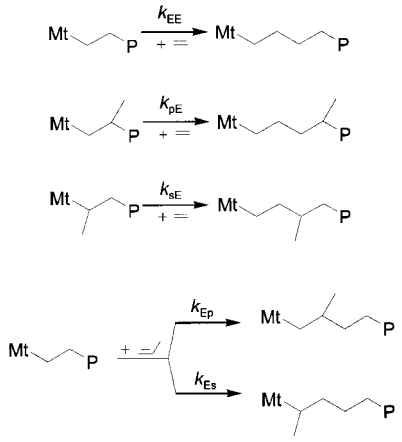

For highly regioselective catalysts such as the ones investigated here, and for mole fractions of propene in the feed not too close to 1, propene/ethene copolymeri-

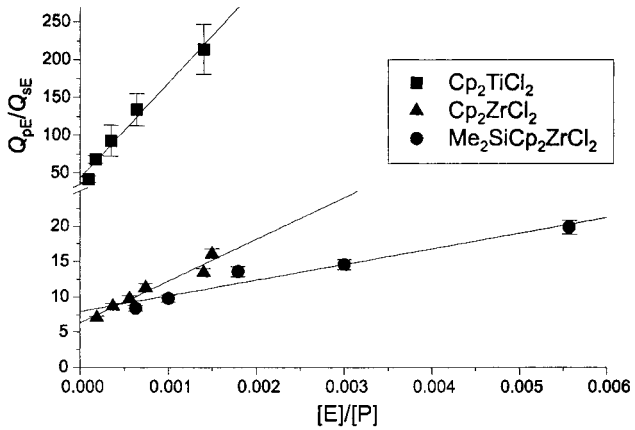

Figure 2. Ratio of ethene-[1-^{13}C] units following a 1,2- or 2,1-propene unit (Q_{pE}/Q_{sE}) vs comonomer feeding ratio in the liquid phase ([E]/[P]) for propene/ethene-[1-^{13}C] copolymers obtained at −15 °C.

Table 4. Normalized Diad and Triad Distributions for Propene/Ethene Copolymers, along with Best-Fit Values of the Reactivity Ratios[a,b]

catalyst	Cp_2TiCl_2	Cp_2ZrCl_2	$Me_2Si(Cp)_2ZrCl_2$
[E]/[P][c]	0.046(2)	0.040	0.083(2)
PP	0.12	0.28	0.49
PE	0.60	0.63	0.48
EE	0.28	0.09	0.04
PPP	0.05	0.19	0.42
PPE	0.14	0.17	0.16
EPE	0.21	0.21	0.12
PEP	0.17	0.25	0.22
EEP	0.28	0.14	0.07
EEE	0.16	0.03	0.01
$r_E = k_{EE}/k_{EP}$	21	7.3(3)	2.1
$r_P = k_{PP}/k_{PE}$	0.020	0.0365(5)	0.19

[a] Determined according to ref 20. [b] Uncertainty of ±1 on the last digit, unless indicated otherwise. [c] E = ethene; P = propene; concentrations in the liquid phase were estimated from the composition of the gas feed according to ref 49.

zation can be treated as binary. Therefore, a "conventional" ^{13}C NMR determination of the reactivity ratios $r_E = k_{EE}/k_{EP}$ and $r_P = k_{PP}/k_{PE}$ (E = ethene, P = propene)[20] can be informative in molecular terms, because propene insertion can be considered as fully 1,2, and therefore it can be set:

$$r_E = k_{EE}/k_{EP} \approx k_{EE}/k_{Ep}$$

$$r_P = k_{PP}/k_{PE} \approx k_{pp}/k_{pE}$$

We thought it worthwhile to prepare, for each catalyst system and at the same temperature of −15 °C, a propene/ethene copolymer at natural isotopic abundance and nearly equimolar incorporation of the comonomers, and to measure r_E and r_P from the normalized ^{13}C NMR distributions of the constitutional diads and triads (Table 4), as described in the literature.[20] The results are given in the last two rows of Table 3. It can be seen that, in all cases, $1/r_P$ is reasonably close to k_{pE}/k_{pp} estimated from the characterization of the propene/ethene-[1-^{13}C] copolymers. The value of r_E, in turn, is only slightly lower than that of the ratio k_{pE}/k_{pp}, which indicates that the relative reactivity of ethene and propene at growing chains with an ethene or a 1,2-propene last-inserted unit is similar.

Finally, we note that the product $(k_{pE}/k_{sE})(k_{sp}/k_{ps})$ is related with catalyst "dormancy". Indeed, in previous papers from this laboratory[16,17] it was shown that, in propene homopolymerization (at least under conditions of negligible chain transfer and isomerization), the fraction C_s* of "dormant" sites with a 2,1-last-inserted propene unit is given by

$$C_s^* = (1 + k_{sp}/k_{ps})^{-1} \quad (3)$$

Unfortunately, there is no experimental way to measure separately the ratios k_{sp}/k_{ps} and k_{pE}/k_{sE}. However, in the following section, we shall see that our quantum mechanical calculations suggest the latter ratio to be not far from unity. We will return to this point and its implications later on.

We conclude this section with a comment on the enantio- (stereo-) selectivity of propene insertion. At the chosen temperature of −15 °C, we confirmed that the homopolymer of propene obtained with Cp_2TiCl_2/MAO is weakly isotactic (fraction of *meso* diads, $[m] \approx 0.7$) due to chain-end control. Concerning the two zirconocenes, the unbridged one also gave some enrichment in *m* diads ($[m] \approx 0.6$), whereas the polypropylene produced with $Me_2SiCp_2ZrCl_2$/MAO turned out to be practically atactic ($[m] \approx 0.5$). It is reasonable to trace this progressive fade of stereoselectivity along the series Cp_2TiCl_2−Cp_2ZrCl_2−$Me_2SiCp_2ZrCl_2$ to a corresponding decrease of steric hindrance at the transition metal. However, even for the titanocene the extent of the asymmetric induction is really small ($\Delta G^{\ddagger} < 1$ kcal/mol); this means that investigating this trend theoretically would be practically meaningless.[34] Moreover, a study of chain-end control would require chain models much larger than the ones we use here. Therefore, catalyst enantioselectivity will not be considered further for these achiral systems.

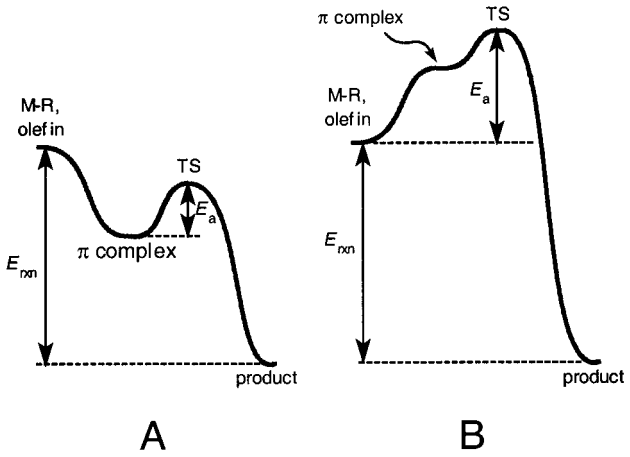

Figure 3. Schematic representation of olefin insertion profile for (A) gas phase and (B) solution with counterion.

2. Calculation of Selectivities: Comparison with Experiment. (a) Solvation/Counterion Effects. The effects of counterion and solvent have to be taken into account somehow to allow prediction of selectivities. Without these effects, most insertion transition states are below the level of the separated reactants, and in solution the activation energies would be energy differences between transition states and the corresponding olefin complexes (Figure 3A). Recent work by Ziegler,[35] however, showed that in many cases olefin coordination to the solvated metal alkyl cation/counterion pair is *endo*thermic. In that case, the effective activation energies are energy differences between transition states and the solvated metal alkyls (Figure 3B), and olefin complexation becomes irrelevant to the selectivity.

Solvent and counterion were not considered explicitly in our calculations. Including a realistic discrete counterion would make both the size of the calculation and the number of degrees of freedom much too large. Including only the solvent would not be useful, since the experimental polymerizations were carried out under conditions of strong cation−anion interaction.[36] Instead, we have made a rough estimate of the combined effect of solvation and cation−anion interaction by assuming the following, for each system:

- $\{Mt(Et)(ethene)]^+\}_{solv}$ is 6 kcal above $\{Mt(Et)]^+\}_{solv}$ + ethene. This estimate is based on calculations by Ziegler.[35a] The *absolute* value is only important when one wants to make a comparison with experimental *activation energies* (which we do not). The *relative* barriers considered here, instead, are not affected by the choice of value.
- Solvation is the same for all isomeric olefin complexes and transition states.

• Adding a methyl group to either alkyl chain (Et→*i*Pr) or olefin (ethene → propene) decreases solvation by a "fudge factor" of 1 kcal/mol. This choice only affects the relative preference for ethene and propene insertion of each species, and the relative reactivities of ethyl and isopropyl species. The value of 1 kcal/mol is admittedly somewhat arbitrary, but we believe that assuming *no* steric effects would be even worse.[37]

These assumptions allow us to put all reactions of a given alkyl cation on the same energy scale (see Table 1). In the text and tables, we will only refer to the "corrected" values.

Of course, different scenarios than the one shown in Figure 3B might apply, depending, e.g., on the choice of solvent and counterion. If the anion were very weakly coordinating (this is the most likely alternative situation), the olefin complex would probably be lower in energy than the solvated alkyl reactants. In that case, the activation energy should be taken from the most stable olefin complex in the system, and olefin complexation would presumably be a rapid preequilibrium. Relative barriers for insertion into the same alkyl would not be affected, but the small differences in complexation energies would cause some changes in the relative reactivities of primary vs secondary alkyls.

(b) Olefin Insertion: General. For all systems studied, olefin insertion follows the standard Cossee path involving a four-center transition state, similar to that reported by several groups for ethene insertion in cationic metallocene−alkyls.[9,38−40] The ring is always slightly puckered, and in all cases we see an α-CH agostic interaction, as expected. Calculated ethene insertion barriers in both Mt−Et and Mt−*i*Pr bonds (unsolvated, relative to the olefin complex) are low (0−6 kcal/mol), and they are highest for the more open H_2SiCp_2Zr system, in agreement with the results reported by Ziegler for insertion in Mt−Me and Mt−Et bonds.[41] Insertion barriers for propene are a bit higher (we will return to this point later), but the transition state geometries are rather similar. Figure 4 shows calculated transition states for 1,2-propene insertion in the Mt−Et bonds of the three systems, illustrating the increasing openness of the metal environment in the order $Cp_2Ti < Cp_2Zr < H_2SiCp_2Zr$.

(c) 2,1-Insertion (Regioerrors). The regiochemistry of propene insertion is presumably determined by both electronic and steric factors. Very open systems (e.g., V-based Ziegler−Natta catalysts, such as VCl_4 or $V(acac)_3$ (acac = acetylacetonate), in combination with $AlEt_2Cl$[42]) tend to prefer the 2,1-insertion mode, at least after a previous 2,1-insertion. More recently, octahedral nonmetallocene catalysts have been reported which behave similarly.[43]

For propene insertion into a metal−primary alkyl bond, our calculations produce a regioselectivity of 4−5 kcal/mol in favor of 1,2-insertion (Table 5), similar to the 4.9 kcal/mol reported by Morokuma for insertion into Cp_2ZrMe^+;[15] the experimental one is slightly lower (3−4 kcal/mol).

For insertion into $H_2SiCp_2ZrMe]^+$, Morokuma estimated a *steric* preference for 1,2-insertion of 3.4 kcal/mol.[44] If this carries over to our $H_2SiCp_2ZrEt]^+$ system, the *electronic* contribution would be less than 1 kcal/mol. As we shall argue later on, the above steric contribution is probably overestimated. Nevertheless, it appears that the electronic preference (which has been stated to favor 1,2-insertion[44]) cannot be large. For metallocenes, where insertion is always predominantly 1,2, steric factors are probably dominant.

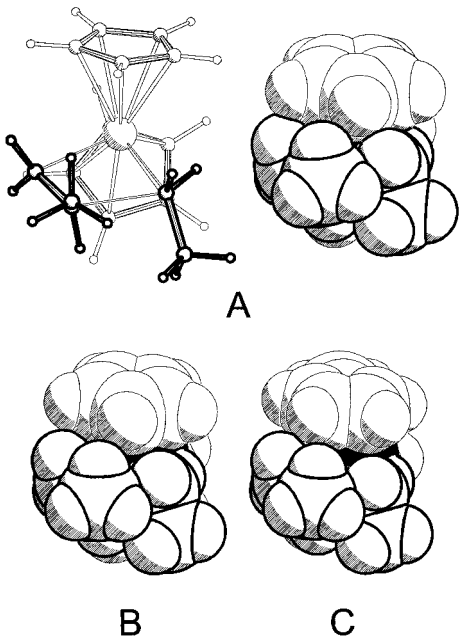

Figure 4. Space-filling models of calculated transition states for 1,2-insertion of propene into the Mt−Et bonds of (A) $Cp_2TiEt]^+$, (B) $Cp_2ZrEt]^+$, (C) $H_2SiCp_2ZrEt]^+$. Visible part of metal atom drawn in black; olefin and alkyl groups are shown with thick outline.

Table 5. Regioselectivity of Propene Insertion (kcal/mol)

	1,2- vs 2,1-insertion in primary alkyl		1,2- vs 2,1-insertion in secondary alkyl
system	$\Delta G^{\ddagger}$(obsd)[a]	$\Delta E_a^{\ddagger}$(calcd)	$\Delta E_a^{\ddagger}$(calcd)[b]
Cp_2Ti	4.32(5)	4.8	1.4
Cp_2Zr	2.96(7)	4.3	1.3
X_2SiCp_2Zr	3.16(7)	4.2	0.7

[a] $RT \ln k_{pp}/k_{ps}$, 1σ error limits. [b] Experimental: $\Delta G^{\ddagger} > 1.2$ kcal/mol.

This being the case, one would expect that regioselectivity parallels the steric properties of the catalyst. Experiment and theory actually agree on Cp_2Ti being the most regioselective system. On the other hand, the two Zr systems have rather similar regioselectivities, with theory suggesting that Cp_2Zr is slightly more regioselective than the bridged homologue, and experiment indicating the opposite (for both sets of numbers, however, the differences are within "error limits"). This is somewhat surprising, since the *ansa*-metallocene is much more open than the unbridged one. Also, the above-mentioned result by Morokuma[44] suggests that even for the Si-bridged system steric effects are still important, so one cannot argue that Cp_2Zr is already so open that further opening would not make a difference. It might be that the expected effect of the more open nature of X_2SiCp_2Zr (X = H or Me) is mostly compensated by the decreased flexibility of the system.

(d) Syn vs Anti Insertion. If propene inserts into a Mt−Et bond, it can do so in two ways: with its methyl group syn or anti to the ethyl C−Me bond. In the achiral systems studied here these would actually lead to the same product and hence cannot be distinguished experimentally, but the distinction becomes important for chiral catalysts. Syn insertion (Figure 5E) is sterically disfavored; we calculate the preference for anti insertion (Figure 5B) to be ca. 4 kcal/mol.

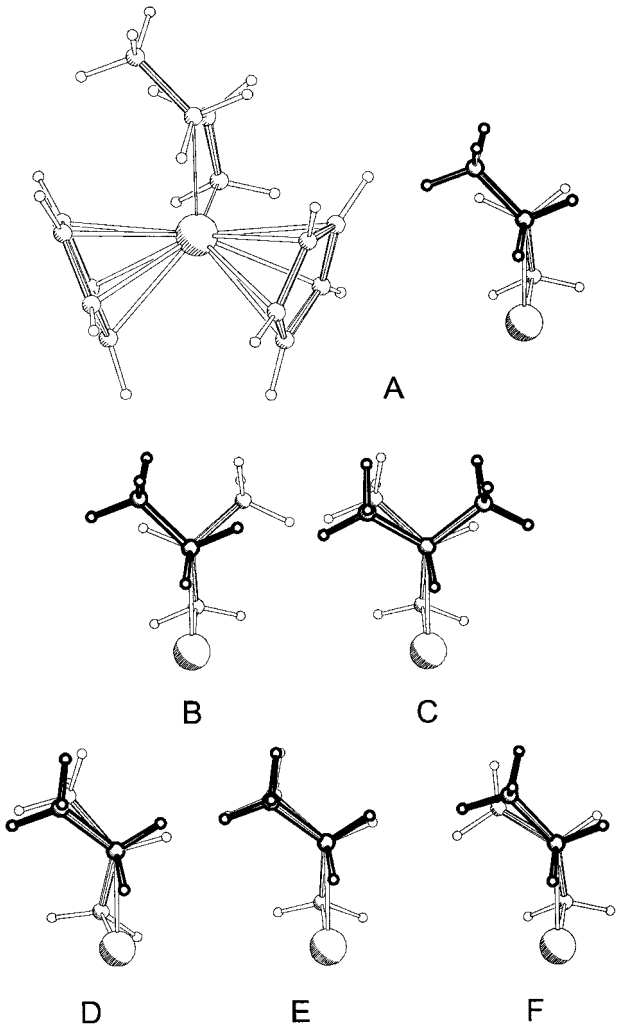

Figure 5. Transition state geometries for (A) Cp_2ZrEt/ethene, (B) Cp_2ZrEt/propene (anti), (C) Cp_2Zr-*i*Pr/propene, (D) Cp_2TiEt/propene (syn), (E) Cp_2ZrEt/propene (syn), (F) H_2SiCp_2ZrEt/propene (syn). Projection is along the alkyl Cα−olefin Cβ halfbond; alkyl group drawn with thick lines.

Actually, the situation is more complex since the alkyl Cα and olefin Cβ carbons are not perfectly eclipsed in the transition state. We *always* observe a puckering of the four-membered transition state that decreases unfavorable syn XC···CY interactions (X, Y = H or Me). Such tilting was already observed by Morokuma in his early study of ethene insertion in Cl_2TiMe^+ (where the chloride was a model for the Cp ligand).[44] For insertion in Mt−Et, the olefin C−Y bond syn to the ethyl C−C bond can move either *in to* or *out of* the ethyl HCC wedge. For ethylene insertion, we always find a movement out of the wedge, as illustrated in Figure 5A; the same movement is observed for anti-insertion of propene (Figure 5B). For syn-insertion of propene, this type of movement would increase steric repulsion of the propene Me group with the Cp groups considerably. As a consequence, we see a gradual shift from out-of movement for the open H_2SiCp_2Zr system to in-to movement for the hindered Cp_2Ti system (Figure 5, parts D−F). For 1,2-propene insertion into the Mt−*i*Pr bond, we find, not surprisingly, that the propene C−Me bond always moves in to the alkyl CCC wedge (Figure 5C).

(e) Consecutive 2,1-Insertions. After a 2,1-insertion, a subsequent 1,2-insertion should be more difficult, since this would connect two tertiary carbons: steric hindrance at the alkyl Cα would compete with hindrance at the metal. As mentioned before, for very open systems, this results in blocks of 2,1-inserted units. For the systems studied here, we predict that the preferred insertion mode is still 1,2, although the preference is strongly reduced (to ca. 1 kcal/mol, see Table 5). As expected, we find the highest selectivity for the more hindered Cp_2Ti system. Experimentally, the percentage of consecutive 2,1-insertions was estimated to be <10% of the total number of regioerrors ($\Delta G^{\ddagger} > 1.2$ kcal/mol).[33]

Table 6. Chemoselectivity of Ethene/Propene Insertion (kcal/mol)

	ethene vs 1,2-propene insertion in primary alkyl		ethene vs 1,2-propene insertion in secondary alkyl	
system	$\Delta G^{\ddagger}$(obsd)[a]	$\Delta E_a^{\ddagger}$(calcd)	$\Delta G^{\ddagger}$(obsd)[b]	$\Delta E_a^{\ddagger}$(calcd)
Cp_2Ti	1.73(5)	2.2	4.10(9)	7.0
Cp_2Zr	1.51(8)	2.4	3.51(8)	5.5
X_2SiCp_2Zr	1.2(1)	2.2	2.89(9)	5.7

[a] $RT \ln k_{pE}/k_{pp}$, 1σ error limits. [b] $RT \ln k_{sE}/k_{sp}$, 1σ error limits.

Table 7. Slowdown of Propene and Ethene Insertion after a 2,1-Insertion (kcal/mol)

	1,2-propene in primary vs secondary alkyl relative to ethene in primary vs secondary alkyl[a]		1,2-propene in primary vs secondary alkyl	ethene in primary vs secondary alkyl
system	$\Delta\Delta G^{\ddagger}$(obsd)[b]	$\Delta\Delta E_a^{\ddagger}$(calcd)	$\Delta E_a^{\ddagger}$(calcd)	$\Delta E_a^{\ddagger}$(calcd)
Cp_2Ti	2.4(1)	4.8	4.7	−0.1
Cp_2Zr	2.0(1)	3.1	2.9	−0.2
X_2SiCp_2Zr	2.1(1)	3.5	3.5	0.0

[a] Values for ethene and propene cannot be measured independently (see text). [b] $RT \ln(k_{pp}/k_{sp})(k_{sE}/k_{pE})$, 1σ error limits.

(f) Ethene vs Propene Insertion: Primary vs Secondary Alkyls. We find that ethene always inserts more easily into a Mt−alkyl bond than propene (Table 6). One should not attach too much significance to the precise energy difference in the table, since the solvation "fudge factor" also contributes to the preference, but even without this, the preference does exist. The difference is much larger for secondary than for primary alkyls, although the calculations seem to exaggerate the difference for secondary alkyls (observed, 3−4 kcal/mol; calculated, 5.5−7 kcal/mol).

Ethene inserts with similar ease into Mt−Et and Mt−*i*Pr bonds (Table 7). Again, the "fudge factor" enters here, but even without it, the difference would be smaller than ca. 1 kcal/mol. Propene, on the other hand, really "feels" the difference between a primary and a secondary alkyl. We attribute this to the fact that with a secondary alkyl it cannot avoid having one unfavorable syn interaction. Thus, propene insertion in a secondary alkyl is estimated to be 3−5 kcal/mol more difficult (a factor 300−10 000 slower) than in a primary alkyl. The comparison between experimental and calculated numbers suggests that the calculations exaggerate the unreactivity of the secondary alkyl toward propene somewhat, and that the real difference should be closer to 2−3 kcal/mol (a factor of 50−300). Nevertheless, the dormancy of a secondary alkyl toward propene insertion is clear enough.

The estimated insensitivity of ethene to the nature of the alkyl group supports its use as a tool for "counting" dormant sites. Indeed, the calculations sug-

Table 8. Key Geometrical Parameters for Transition States (Å)

system	insertion	mode	Mt−C1	Mt−C3	Δ*d*	C2−C3	C1−C3
Cp_2Ti	Et...ethene		2.128	2.485	0.357	1.374	2.418
	Et...propene	1,2 *anti*	2.142	2.391	0.249	1.391	2.392
		1,2 *syn*	2.167	2.302	0.135	1.405	2.350
		2,1 *anti*	2.152	2.461	0.309	1.389	2.248
		2,1 *syn*	2.148	2.489	0.341	1.392	2.277
	*i*Pr...propene	1,2	2.177	2.415	0.238	1.382	2.555
		2,1	2.198	2.465	0.267	1.394	2.289
Cp_2Zr	Et...ethene		2.327	2.463	0.136	1.398	2.310
	Et...propene	1,2 *anti*	2.343	2.393	0.050	1.422	2.254
		1,2 *syn*	2.371	2.342	−0.029	1.430	2.267
		2,1 *anti*	2.342	2.474	0.132	1.413	2.223
		2,1 *syn*	2.339	2.472	0.133	1.414	2.229
	*i*Pr...ethene		2.333	2.567	0.234	1.377	2.531
	*i*Pr...propene	1,2	2.397	2.383	−0.014	1.424	2.340
		2,1	2.383	2.488	0.105	1.410	2.284
H_2SiCp_2Zr	Et...ethene		2.333	2.423	0.090	1.408	2.248
	Et...propene	1,2 *anti*	2.343	2.370	0.027	1.428	2.217
		1,2 *syn*	2.364	2.343	−0.021	1.441	2.219
		2,1 *anti*	2.340	2.443	0.103	1.419	2.184
		2,1 *syn*	2.349	2.430	0.081	1.425	2.180
	*i*Pr...ethene		2.342	2.493	0.151	1.389	2.418
	*i*Pr...propene	1,2	2.390	2.363	−0.027	1.429	2.294
		2,1	2.369	2.469	0.100	1.412	2.256

gest that the ratio k_{pE}/k_{sE} is not far from unity, and that one can therefore set:

$$(k_{pE}/k_{sE})(k_{sp}/k_{ps}) \approx k_{sp}/k_{ps} \quad (4)$$

If that was the case, the fraction of "dormant" sites C_s* could be estimated from the experimental values of $(k_{pE}/k_{sE})(k_{sp}/k_{ps})$ (Table 3, row 3) via eq 3. This would give ≈0.02 for Cp_2TiCl_2/MAO, ≈0.05 for Cp_2ZrCl_2/MAO, and ≈0.09 for $Me_2SiCp_2ZrCl_2$/MAO. All three systems, therefore, would be (much) less dormant than typical bis(Indenyl) *ansa*-zirconocenes (for which it has been reported that C_s* > 0.5).[16,45] This would explain why no appreciable activation of the three catalysts, relative to propene homopolymerization, was observed upon addition of low amounts of ethene-[1-^{13}C] to the feed.

(g) The Flexibility of Transition States. The transition state (TS) for olefin insertion in the Mt−alkyl bond shows considerable flexibility. One would perhaps not expect this for a four-membered ring, but it is important to realize that three of the four ring bonds are only half-bonds. Thus, they can easily respond to changes in the system.

We have already mentioned the variation in staggering of alkyl Cα and olefin C*β* carbons at the TS. Another important variation is seen in the bond lengths within the four-membered ring; Table 8 collects a number of geometrical parameters for the various TS. One aspect of the TS flexibility that can easily be extracted is the variation of the *position* of the TS along the reaction coordinate. This can be characterized by the difference Δ*d* of the lengths of the Mt−C bonds being formed and broken; a more positive value suggests an early TS. The fair inverse correlation between this parameter and the length of the olefinic bond (Figure 6A) supports this interpretation. The data indicate a clear shift from early to late transition states in the sequence *i*Pr/ethene−Et/ethene, R/1,2-propene−R/2,1-propene (R = Et or *i*Pr); this is in accord with the observation by Morokuma of a later transition state for propene insertion into Cp_2ZrMe^+ than for ethene.[15] Also, the TS becomes later in the sequence $Cp_2Ti-Cp_2Zr-H_2SiCp_2Zr$. Both trends appear to be caused by steric effects. In the more hindered metallocenes, steric hindrance between the Cp ligands and the incoming olefin manifests itself early in the reaction but does not increase much once the olefin has entered the coordination sphere. However, steric repulsion between alkyl and olefin peaks later in the reaction, so if that is more important a later TS results.

The length of the C−C bond being formed covers a range of nearly 0.4 Å. Moreover, it does not correlate at all with Δ*d* (Figure 6B), probably because it is influenced both *indirectly* (via the TS position) and *directly* (via steric hindrance between alkyl and olefin) by the substituents. This illustrates the difficulty in assuming a fixed TS geometry for a series of insertion reactions. One would generally expect to find smaller regio- and stereodifferentiation with optimized transition states than with partially frozen ones, since strong steric repulsions will generally be relieved by deformation. Indeed, the regiodifferentiation energies calculated by

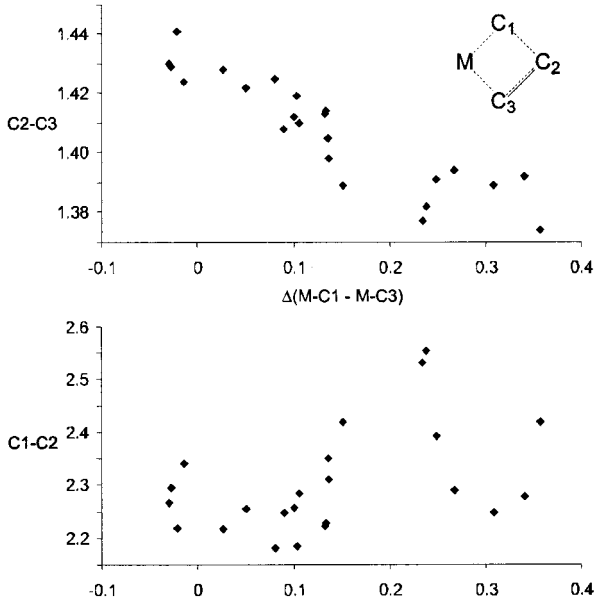

Figure 6. Variation of C2−C3 and C1−C2 bond lengths as a function of Δ*d* (Å units).

Morokuma on the basis of frozen TS geometries[11] are about a factor of 2 higher than our values for comparable systems, and the same seems to be true for stereodifferentiation.[18]

Conclusions

The main purpose of this work was not to predict all possible insertion selectivities to very high accuracy from first principles. Such a calculation would presumably require explicit solvent and counterion models, much larger basis sets, larger chain models, and unconstrained optimization of ligand structures, as well as contribution of dynamic effects; we believe that this is not yet feasible. However, even with the admittedly crude approximations made here, we can already achieve a rather satisfactory agreement between experiment and theory. This indicates that solvent and counterion effects, though undoubtedly important, are rather indiscriminate, at least for the catalysts and reaction conditions considered here.[46] It also strongly suggests that olefin insertion is the rate-determining step on the reaction path (i.e. the insertion transition state is the highest point of the path); if, for example, olefin coordination were rate-determining, this would also determine the ethene/propene selectivity, and there would be no reason the trends in "coordination barriers" would parallel our calculated insertion barriers. Thus, the current work provides justification for using relative insertion barriers to predict chemo-, regio-, and stereoselectivities for other systems.

Comparison of the "reference" Cp_2Zr/Et/ethene system with other prototypical ones involving a different transition metal center, chain, or olefin reveals three important effects:

- Space around the metal center increases in the order $Cp_2Ti < Cp_2Zr < X_2SiCp_2Zr$.[47] Discrimination between 1,2- and 2,1-propene insertion decreases clearly between Cp_2Ti and Cp_2Zr, but unexpectedly, we do not see much further loss of regioselectivity on going to X_2SiCp_2Zr (X = H, Me).
- Propene insertion (with *any* regiochemistry) is always more difficult than ethene insertion.
- Propene insertion is particularly difficult if there is a syn orientation between olefin C−Me bond and alkyl chain.

The theoretical results fully support the dormant site hypothesis for secondary alkyls,[2,16,17] originally proposed on the basis of experimental evidence. They also suggest that insertion of ethene, in contrast to propene, is *not* hindered at a secondary alkyl, and thus they provide additional justification for the use of propene/ethene copolymerization as a method for measuring not only the regioselectivity of propene insertion[2] but also the fraction of dormant sites in propene homopolymerization.[48]

Acknowledgment. V.B. and R.C. acknowledge the Italian Ministry for University (PRIN 2000) and P.B. acknowledges the Dutch Polymer Institute (DPI Project no. 104) for financial assistance. The NMR characterization of all copolymers was carried out at the "Centro di Metodologie Chimico-Fisiche" of the University of Naples "Federico II".

Supporting Information Available: Scheme showing all the possible chain propagation steps in a propene/ethene copolymerization, text giving the derivation of eq 2, and a table showing total energies for all species mentioned in the text (Table S1) (4 pages). Optimized geometrical parameters for all species are available on request from P.B. This material is available free of charge via the Internet at http://pubs.acs.org.

References and Notes

(1) Busico, V.; Cipullo, R. *Prog. Polym. Sci.* **2001**, *26*, 443.
(2) Busico, V.; Cipullo, R.; Talarico, G.; Caporaso, L. *Macromolecules* **1998**, *31*, 2387.
(3) (a) Busico, V.; Cipullo, R.; Esposito, V. *Macromol. Rapid Commun.* **1999**, *20*, 116. (b) Liu, Z.; Somsook, E.; Landis, C. R. *J. Am. Chem. Soc.* **2001**, *123*, 2915.
(4) (a) Brintzinger, H. H.; Fischer, D.; Mülhaupt, R.; Rieger, B.; Waymouth, R. M. *Angew. Chem., Int. Ed. Engl.* **1995**, *34*, 1143. (b) Resconi, L.; Cavallo, L.; Fait, A.; Piemontesi, F. *Chem. Rev.* **2000**, *100*, 1253.
(5) Albizzati, E.; Giannini, U.; Collina, G.; Noristi, L.; Resconi, L. Catalysts and Polymerizations. In *Polypropylene Handbook*; Moore, E. P. Ed.; Hanser Verlag: Munchen, Germany, 1996.
(6) For recent reviews, see: (a) Rappé, A. K.; Skiff, W. M.; Casewit, C. J. *Chem. Rev.* **2000**, *100*, 1435. (b) Angermund, K.; Fink, G.; Jensen, V. R.; Kleinschmidt, R. *Chem. Rev.* **2000**, *100*, 1457.
(7) See, e.g., (a) Fusco, R.; Longo, L.; Masi, F.; Garbassi, F. *Macromolecules* **1997**, *30*, 7673. (b) Fusco, R.; Longo, L.; Proto, A.; Garbassi, F. *Macromol. Rapid. Commun.* **1998**, *19*, 257. (c) Lanza, G.; Fragalà, I. L.; Marks, T. J. *J. Am. Chem. Soc.* **1998**, *120*, 8257. (d) Chan, M. S. W.; Ziegler, T. *Organometallics* **2000**, *19*, 5182.
(8) Margl, P.; Lohrenz, J. C. W.; Ziegler, T.; Blöchl, P. E. *J. Am. Chem. Soc.* **1996**, *118*, 4434.
(9) Kawamura-Kuribayashi, H.; Koga, N.; Morokuma, K. *J. Am. Chem. Soc.* **1992**, *114*, 8687.
(10) Castonguay, L. A.; Rappé, A. K. *J. Am. Chem. Soc.* **1992**, *114*, 5832.
(11) Yoshida, T.; Koga, N.; Morokuma, K. *Organometallics* **1996**, *15*, 766.
(12) Sakai, S. *Int. J. Quantum Chem.* **1997**, *65*, 739.
(13) See Michalak, A.; Ziegler, T. *Organometallics* **2000**, *19*, 1850 for a similar QM/MM study on ethene and propene polymerization at late transition metals (Ni, Pd).
(14) Moscardi, G.; Resconi, L.; Cavallo, L. *Organometallics* **2001**, *20*, 1918.
(15) Froese, R. D. J.; Musaev, D. G.; Morokuma, K. *J. Mol. Struct. (THEOCHEM)* **1999**, *461*−*462*, 121.
(16) (a) Busico, V.; Cipullo, R.; Corradini, P. *Makromol. Chem., Rapid Commun.* **1993**, *14*, 97. (b) Busico, V.; Cipullo, R.; Chadwick, J. C.; Modder, J. F.; Sudmeijer, O. *Macromolecules* **1994**, *27*, 7538. (c) Busico, V.; Cipullo, R. *Macromol. Symp.* **1995**, *89*, 277.
(17) (a) Busico, V.; Cipullo, R.; Corradini, P. *Makromol. Chem., Rapid Commun.* **1992**, *13*, 15. (b) Busico, V.; Cipullo, R.; Corradini, P. *Macromol. Chem.* **1993**, *194*, 1079.
(18) Borrelli, M.; Busico, V.; Cipullo, R.; Ronca, R.; Budzelaar, P. H. M. Manuscript in preparation.
(19) Cheng, H. N.; Smith, D. A. *Macromolecules* **1986**, *19*, 2065.
(20) Kakugo, M.; Naito, Y.; Mizunuma, K.; Miyatake, T. *Macromolecules* **1982**, *15*, 1150.
(21) GAMESS−UK is a package of ab initio programs written by M. F. Guest, J. H. Van Lenthe, J. Kendrick, K. Schoffel, and P. Sherwood, with contributions from R. D. Amos, R. J. Buenker, H. J. J. Van Dam, M. Dupuis, N. C. Handy, I. H. Hillier, P. J. Knowles, V. Bonacic-Koutecky, W. Von Niessen, R. J. Harrison, A. P. Rendell, V. R. Saunders, A. J. Stone, and A. H. De Vries. The package is derived from the original GAMESS code due to: Dupuis, M.; Spangler, D.; Wendoloski, J. *NRCC Software Catalog*; 1980, Vol. 1, Program No. QG01 (GAMESS). DFT module by P. Young, under the auspices of EPSRC's Collaborative Computational Project No. 1 (CCP1) (1995−1997).
(22) (a) Lee, C.; Yang, W.; Parr, R. G. *Phys. Rev. B* **1988**, *37*, 785. (b) Becke, A. D. *J. Chem. Phys.* **1993**, *98*, 1372. (c) Becke, A. D. *J. Chem. Phys.* **1993**, *98*, 5648.
(23) Binkley, J. S.; Pople, J. A.; Hehre, W. J. *J. Am. Chem. Soc.* **1980**, *102*, 939.
(24) Hehre, W. J.; Stewart, R. F.; Pople, J. A. *J. Chem. Phys.* **1969**, *51*, 2657.
(25) (a) Hay, P. J.; Wadt, W. R. *J. Chem. Phys.* **1985**, *82*, 270. (b) Wadt, W. R.; Hay, P. J. *J. Chem. Phys.* **1985**, *82*, 284. (c) Hay, P. J.; Wadt, W. R. *J. Chem. Phys.* **1985**, *82*, 299.
(26) This choice of basis set is identical to the one used in ref 11; for the metal and reactive part, it is nearly equivalent to the

one used in ref 15. Ligand C−C distances are about 0.01 Å longer than those calculated with the a double-ζ basis,[15] and vary less than 0.01 Å over the reaction path.

(27) We are currently evaluating the effects of choice of basis set, functional (DFT) or correlation method (post-Hartree−Fock) in-depth for the model system Cp_2Zr as well as two constrained-geometry catalysts: Cavallo, L.; Blok, A. N. J.; Talarico, G.; Budzelaar, P. H. M. To be submitted for publication.

(28) We have verified the nature of each transition state by a second-derivative calculation. However, since geometry restrictions were used the calculated "frequencies" do not correspond directly to normal modes, so the resulting ZPE and thermal corrections would not be meaningful. ZPE corrections to barrier heights are expected to be on the order of a few kilocalories per mole. However, in the present context, we are only using *relative* barriers for very similar reactions; the errors in these should be much smaller, well within the margins of other sources of error.

(29) (a) Natta, G.; Pino, P.; Mazzanti, G.; Giannini, U. *J. Inorg. Nucl. Chem.* **1958**, *8*, 612. (b) Breslow, D. S.; Newburg, N. R. *J. Am. Chem. Soc.* **1957**, *79*, 5073. (c) Andresen, A.; Cordes, H. G.; Herwig, J.; Kaminsky, W.; Merck, A.; Mottweiler, R.; Pein, J.; Sinn, H.; Vollmer, H. J. *Angew. Chem., Int. Ed. Engl.* **1976**, *15*, 630.

(30) Ewen, J. A. *J. Am. Chem. Soc.* **1984**, *106*, 6355.

(31) (a) Busico, V.; Mevo, L.; Palumbo, G.; Zambelli, A.; Tancredi, T. *Makromol. Chem.* **1983**, *184*, 2193. (b) Chien, J. C. W.; He D. *J. Polym. Sci., A* **1991**, *29*, 1585. (c) Zambelli, A.; Grassi, A. *Makromol. Chem., Rapid Commun.* **1991**, *12*, 523. (d) Uozumi, T.; Soga, K. *Makromol. Chem.* **1992**, *4*, 193.

(32) Busico, V.; Cipullo, R.; Talarico, G.; Segre, A. L.; Caporaso, L. *Macromolecules* **1998**, *31*, 8720.

(33) Busico, V.; Cipullo, R.; Ronca, S. *Macromolecules*, in press; the relevant argument is supplied as part of the Supporting Information.

(34) For an attempt to explain isotactic chain-end control for Cp_2TiCl_2 on the basis of MM models, see: Venditto, V.; Guerra, G.; Corradini, P.; Fusco, R. *Polymer* **1990**, *31*, 530.

(35) (a) Chan, M. S. W.; Vanka, K.; Pye, C. C.; Ziegler, T. *Organometallics* **1999**, *18*, 4624. (b) Vanka, K.; Chan, M. S. W.; Pye, C. C.; Ziegler, T. *Organometallics* **2000**, *19*, 1841.

(36) Beck, S.; Lieber, S.; Schaper, F.; Geyer, A.; Brintzinger, H.-H. *J. Am. Chem. Soc.* **2001**, *123*, 1483.

(37) As an indication, the Zr−B distances in $[Me_2SiCp_2Zr(Et)(ethene)]^+[B(C_6F_5)_4]^-$ and $[Me_2SiCp_2Zr(Et)(propene)]^+[B(C_6F_5)_4]^-$ are calculated as 7.54 and 7.76 Å at the PM3 level. If we put the centers of unit positive and negative charge at the Zr and B atoms, this corresponds to a change in electrostatic interaction of 1.2 kcal/mol.

(38) Weiss, H.; Ehrig, M.; Ahlrichs, R. *J. Am. Chem. Soc.* **1994**, *116*, 4919. These authors did not find a discrete transition state along the reaction path, but the geometries of intermediate points of the path were very similar to those expected for the "Cossee" π-complex.

(39) Woo, T. K.; Fan, L.; Ziegler, T. *Organometallics* **1994**, *13*, 2252.

(40) For ethene insertion into $Cp_2Ti\textit{i}Pr]^+$, the insertion is (virtually) barrierless.

(41) See, e.g.: Margl, P.; Deng, L.; Ziegler, T. *J. Am. Chem. Soc.* **1998**, *120*, 5517 and references cited there.

(42) See, e.g.: (a) Natta, G.; Pasquon, I.; Zambelli, A. *J. Am. Chem. Soc.* **1962**, *84*, 1488. (b) Zambelli, A.; Tosi, C.; Sacchi, C. *Macromolecules* **1972**, *5*, 649.

(43) (a) Tian, J.; Coates, G. W. *Angew. Chem., Int. Ed. Engl.* **2000**, *39*, 3626. (b) Tian, J.; Hustad, P. D.; Coates, G. W. *J. Am. Chem. Soc.* **2001**, *123*, 5134. (c) Saito, J.; Mitani, M.; Onda, M.; Mohri, J.-I.; Ishii, S.-I.; Yoshida, Y.; Nakano, T.; Tanaka, H.; Matsugi, T.; Kojoh, S.-I.; Kashiwa, N.; Fujita, T. *Macromol. Rapid Commun.* **2001**, *22*, 1072. (d) Lamberti, M.; Pappalardo, D.; Zambelli, A.; Pellecchia, C. *Macromolecules* **2002**, *35*, 658.

(44) Kawamura-Kuribayashi, H.; Koga, N.; Morokuma, K. *J. Am. Chem. Soc.* **1992**, *114*, 2359.

(45) We believe that the higher dormancy of isospecific catalysts is directly related to the stereoregulation mechanism. A detailed explanation will be given in ref 18.

(46) Indeed, counterion/solvent effects on regioselectivities of metallocene catalysts have never been reported.

(47) (a) Cp_2Ti vs Cp_2Zr: Margl, P.; Deng, L.; Ziegler, T. *Organometallics* **1998**, *17*, 933. (b) Cp_2Zr vs H_2SiCp_2Zr: ref 39.

(48) Due to the possible occurrence of chain transfer and/or isomerization of 2,1- into 3,1-units, catalyst dormancy may be somewhat lower than that estimated on the basis of relative monomer insertion rates only.

(49) Kissin, Y. V. *Isospecific Polymerization of Olefins*; Springer-Verlag: New York, 1985; p 3.

MA011557H